Results in Control and Optimization 12 (2023) 100294

Contents lists available at ScienceDirect

Results in Control and Optimization

journal homepage: www.elsevier.com/locate/rico

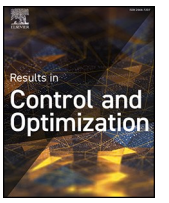

# A platform for demand response and intentional islanding in distribution grids: The LIVING GRID demonstration project

Remon Bekhit [d], Giovanni Bianco [a], Federico Delfino [a], Giulio Ferro [a,*], C. Noce [b], Luca Orrù [d], Luca Parodi [a], Michela Robba [a], Mansueto Rossi [a], Giovanni Valtorta [c]

[a] University of Genova, Genova 16145, Italy
[b] Enel-X, Italy
[c] Enel Distribuzione (Distribution System Operator), Italy
[d] TERNA, Innovation Factory System Operator (Transmission System Operator), Italy

ARTICLE INFO

*Keywords:*
Energy management system
Optimization
Distribution system operator
Transmission system operator
Smart grids
Islanding

ABSTRACT

An optimization-based platform is presented to request ancillary services and perform demand response. The work has seen a joint effort of the Italian TSO and DSO (Transmission and Distribution System Operators) and active local prosumers within the LIVING GRID innovation and demonstration project. The platform, a pure software architecture based on existing control and supervision equipment in the prosumer's plant, embeds optimization models, can communicate reference values for active and reactive power and perform intentional islanding and demand response in portions of the distribution grid and microgrids. Two possible configurations have been tested: Single PoC (Point of Connection) and Multi-PoC. The results of the optimization model and in-field experiments are presented and discussed for the considered pilot site: the Savona Campus Smart Polygeneration Microgrid (University of Genova, Italy).

## 1. Introduction

The rapid growth of intermittent renewable energy resources and distributed generation has necessitated the development of new controllers and management techniques for smart grids. This is due to the challenges posed by voltage and frequency fluctuations caused by renewable sources, which negatively impact the power system. Additionally, the increased modulation required from large fossil fuel generation plants to accommodate renewables affects the operational life of their components. Furthermore, the complexity of the situation is amplified by the rise of small and distributed generators, potentially involving millions of producers in ancillary services and energy markets.

To address these challenges, new players and technologies have emerged, including Aggregators and innovative information and communication technology (ICT) platforms. For instance, an Aggregator can coordinate and reduce customers' energy demand to alleviate congestion and emergencies in the power grid. In some cases, specific sections of the distribution grid may need to operate in islanded mode. Consequently, grid operators, such as the Transmission System Operator (TSO) and the Distribution System Operator (DSO), are expanding their roles and incorporating new tools into existing ICT platforms. This facilitates the transition of the power grid towards more flexible electrical systems, necessitating data management, remote control capabilities, and accurate forecasting of renewable production, demands, and flexibility [1–4].

* Corresponding author.
*E-mail address:* giulio.ferro@unige.it (G. Ferro).

https://doi.org/10.1016/j.rico.2023.100294
Received 10 March 2023; Received in revised form 30 June 2023; Accepted 5 September 2023
Available online 9 September 2023

**Acronyms**

| | |
|---|---|
| DSO | distribution system operator |
| TSO | transmission system operator |
| ARERA | Italian regulatory authority for energy, networks and environment |
| BESS | battery energy storage system |
| CHP | combined heat and power |
| CNR | national council of research |
| DER | distributed energy resource |
| DERMS | distributed energy resources management system |
| DR | demand response |
| EMS | energy management system |
| EnSiEL | national inter-university centre on power systems |
| GHP | geothermal heat pumps |
| HVAC | heating, ventilation and air conditioning |
| ICT | information and communication technology |
| MPC | model predictive control |
| MV/LV | medium voltage/low voltage |
| PoC | point of connection |
| PV | photovoltaic |
| RSE | research for the energy system |
| SCADA | supervisory control and data acquisition |
| SEB | smart energy building |
| SPM | smart polygeneration microgrid |
| VEN | virtual end node |
| VTN | virtual top node |

Microgrids, which represent sustainable districts and portions of the electrical grid, require dedicated local Energy Management Systems (EMS). These systems are essential for forecasting and communicating flexibility boundaries in the day-ahead market or automatically managing on-field operations based on signals from the DSO. Test-beds play a crucial role in demonstrating the effectiveness and applicability of models, methods, and tools within this framework [5].

The ability to deliver ancillary services to transmission network operators has been extended to a wide range of end-users, thanks to the emergence of new balancing service providers like Aggregators. These providers can manage the flexibility of numerous small customers and offer it to System Operators. In Italy, this opportunity was initially explored through pilot projects [6] and has now reached a mature stage.

However, there are several outstanding issues that require attention, including coordination between the DSO and TSO and the DSO's access to local flexibility services. Currently, in Italy, only the TSO can participate in ancillary services and balancing markets, while the DSO can request customer modulating actions for safety reasons only, specifically when the secure operation of the distribution network is at risk. Recently, following the publication of the EU Directive 2019/944 [7] and its transposition into Italian regulation, pilot projects have been initiated by the Italian Regulatory Authority for Energy, Networks, and Environment (ARERA) to explore the delivery of local flexibility services to the DSO [8].

Numerous papers have proposed and analysed potential structures for a local ancillary services market [9,10]. However, this paper focuses on evaluating the technical feasibility of a platform that enables both the DSO and TSO to request flexibility actions from active users connected to a local distribution network.

The experimental activity presented in this paper was conducted within the scope of the LIVING GRID project (2017–2020) of the Italian Technological Innovation Cluster on Energy. The project involved several partners, including ENEA (Italian Energy and Environmental Agency), TERNA (Italian TSO), e-distribuzione (Italian DSO), RSE (Research for the Energy System), CNR (National Council of Research), and EnSiEL (National Inter-University centre on power systems, with research units from the University of Genova, Polytechnic of Torino, and Polytechnic of Bari).

The main objective of the LIVING GRID project was to develop and test a prototype ICT architecture that enables operators from both the DSO and TSO to input flexibility requests to prosumers for specific time periods. These requests include constraints on active and reactive powers at specific buses and temporary constraints on power flows along lines. The platform then relays these requests to the available assets of active customers connected to a local distribution network, such as generators or demand response actions utilizing manageable loads.

Furthermore, the aim of the project was to test the feasibility of a purely software architecture, only relaying on control and supervision equipment already present in the prosumer's plant, without the need to install additional hardware at the prosumer premises. This particular activity was carried out by Terna, e-distribuzione, and the University of Genoa.

Two scenarios were considered to assess the architecture, involving different types of active customers with varying complexities and capabilities. In one scenario, requests from the DSO/TSO were directly sent to assets like PV fields or a storage device, simulating

the case of small customers with only one asset each. In the other scenario, the platform sent requests to the Energy Management System (EMS) of a microgrid, representing a more complex user. This case also tested the possibility of requesting the islanding of a portion of the microgrid. An EMS specifically designed for this project, capable of considering the flexibility requests from the platform, was developed for the second scenario.

Additionally, one of the objectives of this activity was to verify whether the platform could operate using existing communication links and protocols provided by the assets involved, such as photovoltaic systems, storage devices, microturbines, HVAC systems, and the SCADA (Supervisory Control And Data Acquisition) system of the microgrid, without requiring additional communication, metering, and control equipment installations.

The demonstration activities described in the paper took place at the pilot site of the Savona Campus SPM. This site features a 3-phase low voltage (400 V line-to-line) "intelligent" distribution system connected to a thermal network composed of electrical/thermal loads and generation units, including microturbines, photovoltaics, and heat pumps. The SPM's electrical grid topology consists of a ring with one main switchboard and five other switchboards connected to power plants, loads, and a Smart Energy Building (SEB). Key devices in the SPM include two cogeneration gas microturbines, three photovoltaic generation plants, an electrical storage system, absorption chillers, and a gas boiler. The SPM is controlled and managed by an ICT system comprising field data acquisition and local automation devices, a SCADA system, and remote terminal units acting as local controllers for a subset of plants. Communication protocols based on IEC 61,850, Modbus, and Bacnet are used to communicate with plants and sensors.

In summary, the main contributions of the paper are as follows:

- Definition of a platform's architecture jointly developed and tested by the key stakeholders in the smart grid (TSO, DSO, active local prosumers) for demand response and intentional islanding.
- Introduction of a new optimization model for selecting the optimal schedule of production plants and storage systems and/or intentionally islanding a portion of the grid.
- Description of the field tests performed during the National project LIVING GRID by the Italian Technological Innovation Cluster on Energy.

The paper is structured as follows: Section 2 provides an overview of the state of the art, Section 3 presents the developed ICT architecture, Section 4 showcases the results and demonstration activities, and finally, Section 5 concludes the paper.

## 2. State of the art

In the recent literature, several papers deal with demand response (DR), aggregators, EMSs for smart grids [11–13]. Attention is particularly focused on models, methods, and ICT tools for DR. However, most articles do not include the collaboration with DSO and TSO and/or the report on real in-field experiments at a larger scale than the laboratory one.

DR covers one of the most relevant roles in which smart grids are considered profitable. According to [14,15], by improving the reliability of the power system and lowering peak demand, DR can reduce overall plant and capital cost investments and postpone the need for network upgrades. Many of the opportunities and the challenges linked with DR are presented in [16]. As presented in [17], DR is a strategy by which a consumer can play a key role in the operation of the smart grid either by reducing the peak load or shifting the electricity consumption from on-peak to off-peak hours. An interesting approach is presented in [18], where the authors propose a linearized multi-objective robust optimization testing the performances of different DR policies linked with the retailer and consumer costs. A distinction between two classes of DR is also given by [19]: incentive-based DR and price-based DR. In the first case, incentives are provided to the consumers for changing their consumption patterns according to the needs of the utilities. In the second case, the benefits of the wholesale electricity price market are directly passed to consumers to pay for electricity at different times of the day. Amongst the studies that consider incentive-based DR, authors in [20] present a study conducted from a microgrid owner's perspective, aiming to determine the DR incentives for its customers considering the feasibility for both DR participants and the microgrid operator. In the optimization, the authors consider the discomfort of the customers.

Regarding the price-based DR programs, an interesting study is proposed by [21], where the authors present an optimization model based on dynamic price-based DR, including deferrable and non-deferrable loads and renewable sources. The two presented cases solve the problem using particle swarm optimization. Another interesting contribution is given by [22], where the authors present a DR scheduling model for smart residential communities based on load despatch through a load aggregator. The authors optimally schedule the residential loads through their model by combining different price-based DR programs and interruptible loads.

From an ICT point of view, in [23], the authors investigate DERMS (distributed energy resources management system) platforms, which are identified as tools to coordinate DER (Distributed Energy Resource) units and microgrids to enhance the stability of the distribution network and to provide flexibility services. Reilly in [24] describes a DERMS for a microgrid, able to participate in the energy market and the transmission and distribution system operations. More specifically, the presented DERMS allows utilities to control DERs, send the market signal to an aggregate of DERs, and provide ancillary services. The authors in [25] propose a solution to improve the critical load restoration capability of distribution systems using DERs. A two-stage critical load restoration optimization scheme is formulated using DERs control coordination and the DSO-DERMS interaction paradigm. The main difference between [23–25] and the proposed work is that the platform does not only manage the interaction between DERs and TSO or DSO, as in [23–25], but it additionally considers the interaction amongst the DSO and the TSO. Indeed, this platform can be used by TSO to send requests to DERs (Distributed Energy Resources), granted the authorization by the DSO, which verifies and confirms, through the DERMS interface, that the requests of the TSO are compatible with the distribution network operation and constraints.

In the DERMS framework, algorithms play a crucial role in optimizing various operations. In a comprehensive study [26], an innovative real-time algorithm is proposed, specifically designed to tackle optimal power flow and effectively control PV and DERs within large-scale distribution networks. Another noteworthy contribution by Peppanen et al. [27] introduces a tool aimed at controlling the curtailment of PV plants in distribution networks. Their approach employs an iterative load flow algorithm to facilitate control and ensure optimal utilization of resources. Furthermore, in [28], the authors adopt a reverse Stackelberg game-theoretic approach to achieve control over energy systems. This novel approach presents a fresh perspective on managing and optimizing the performance of energy systems. In [29], Morrissey et al. define a bi-level algorithm, in which the higher level provides strategic day-ahead scheduling for the DERs, considering PV and loads forecast, whereas the lower level dispatches in real-time based on updated measurements. Instead, the management platform presented in this paper employs a different approach concerning [26–29]: an MPC (Model Predictive Control) algorithm that progressively solves a mixed-integer linear programming optimization problem.

Moreover, two possible control strategies are considered for two different scenarios, called single Point Of Connection (POC) and multi POC. The first algorithm defines the setpoints for an aggregate cluster of DERs, leaving the control strategy of the single unit to a local EMS, whereas the second method directly identifies the signals for each DER unit. From a real application point of view, DERMS platforms are being employed in the US to manage the distributed generation assets [30]. In [31] the authors simulate the response of a DERMS platform (which controls several photovoltaic inverters in a distribution network in California) to cyber-attacks. Also, in the rest of the world DERMS are gaining ground: in [32], the authors define a platform to improve the efficiency of flexibility provision in an MV-LV grid, and the operation is simulated on the real structure of MV and LV networks of a Swiss DSO, determining that the DSO operation costs can be reduced thanks to the increase of the available flexibility. Ahmadi et al. [33] present simulation results regarding using a DERMS platform to control the interaction between DERs and the UK distribution network. The study considers active and reactive power services provided to the national grid, and it demonstrates that DERMS can control DERs operation to achieve grid requirements at the POC by procuring the cheapest resources available. In the present work, the presented platform is applied to the Italian distribution network: it is one of the first attempts in Italy to implement a platform that allows both the DSO and TSO to perform coordinated requests to DERs or a microgrid, tested on a real-world infrastructure.

In many cases, the DERMS applications are not yet ready to be tested in the field, and therefore they are validated in a simulation environment. In [34], Padullaparti et al. propose a DERMS based on real-time optimal power flow, able to control BESS (Battery Energy Storage System) to reduce the power request during high demand hours providing a peak shaving service. In [35] a platform to manage the high penetrations of PV units on a distribution network is presented and validated through simulation based on real data. In [36], Nowak et al. propose a platform to connect a DSO to a cluster of DERs through an IoT appliance, and simulation scenarios to confirm the sanity of the DERMS are presented.

Differently from [34–36], in the present paper, the developed DERMS is validated using experimental field tests with the participation of both the TSO and DSO authorities.

## 3. The developed ICT architecture

The developed platform ("DSO platform" as it acts on resources on the distribution network, although TSO operators can also access it) allows a procedure through which the flexibility requests can be formulated, validated, and applied in field. Specifically the following actions have been performed during the project:

- a baseline for active and reactive power fluxes during the day was computed based on load forecast, generation forecast, and current generation planning for the dispatchable resources; in addition, flexibility margins for the assets were also estimated;
- TSO operators could specify constraints on active/reactive power exchanged by the portion of the distribution network or specify variations to the baseline in given periods;
- TSO requests were validated by the DSO (which has the actual visibility of the distribution network);
- DSO operators could also formulate requests in terms of constraints on active and reactive powers at specific buses, temporary constraints on power fluxes along lines, variations with respect to the baseline, or requesting the islanding of a subset of the customer's network;
- the requests were then translated into new setpoints for the available assets and sent to them.

As previously mentioned in the introduction, two scenarios were considered:

- *Scenario 1 (Single-PoC)*. The microgrid is viewed as a single client receiving active and reactive power signals. In this case, the DSO/microgrid interface allows commands to be sent, and it is the microgrid EMS that optimally schedules plants and components. The EMS aggregates all the Savona Campus plants and is based on optimization models and able to: a) guarantee the operational management of the plants; b) manage the microgrid by considering active and reactive power signals from the DSO platform; c) manage the microgrid in case of islanding of a portion of the microgrid. In this scenario, the requests for flexibility services can be issued both by the TSO and the DSO.
- *Scenario 2 (Multi-PoC)*. Each generation and storage facility in the microgrid is viewed as a single user part of the distribution network: the microgrid is used to "mimic" a distribution feeder to which several users are connected. In this case, the DSO, by means of the platform, directly sets the setpoints for each device, and issues load shedding requests.

In the following, both Scenarios would be described and the mathematical formulation of the EMS would be stated.

### 3.1. Scenario 1: Single PoC

The Single PoC configuration (see Fig. 1) describes the actual operation of the Campus, considered as a single user with different kinds of flexibility (i.e., battery, GHPs (Geothermal Heat Pumps), islanded operation, electric vehicles).

The architecture is characterized by the following functionalities: (a) the use of the DSO's platform that acts as a VTN (Virtual Top Node), through the OpenADR communication protocol, to set constraints at the Campus connection point (e.g. maximum active/reactive power, required active power value, etc.) that will result in flexibility requests (set by both TSO and DSO); (b) a Virtual End Node (VEN), which receives the flexibility requests from the DSO platform in OpenADR format, that interfaces with the Campus EMS; the same VEN sends to the DSO platform the flexibility made available for the following day, according to the time schedule of the micro-network, and reports on measurements; (c) the EMS installed at the Campus, which computes the optimal scheduling of the programmable resources of the microgrid, considering the flexibility requests at the connection point, and sends setpoints to the devices (by the use of different communication protocols: Modbus, BACnet, or IEC61850, as reported in Fig. 2).

To carry out the transition tests in islanded mode and return to parallel mode with the network, the control of the Campus resources is carried out by the SCADA (e.g., the stopping of the storage system and its restarting in V/f mode (voltage and frequency control), the opening of the parallel switch and its reclosing with synchronism control). Therefore, in this case, the island request is transmitted from the DSO platform to the EMS, translating it into IEC61850 commands, received by SCADA via OPC through a specially configured IEC61850-OPC Gateway (see Fig. 3).

### 3.2. Scenario 2: Multi PoC

In this second scenario, the individual nodes of the Smart Polygeneration Microgrid (SPM) are considered independent customers connected to the LV distribution network (see Fig. 4). In this way, interactions with DERs simpler than a microgrid (such as households equipped with PV) can be tested.

From the architecture point of view, in this case, the EMS does not perform any action; the commands from the platform are directly sent to the RTUs, thus emulating the direct access between the DSO platform and distributed customers. Regarding the communication scheme, a direct interface in IEC 61850 has been implemented between the DSO platform and the RTUs (Fig. 5). The SEB, with the PV field installed on it (PV3), is seen by the DSO platform as a single complex user through the EMS, which exchanges information with the DSO platform in OpenADR. The EMS is directly interfaced with the control units that control the SEB in BACnet and the PV system in Modbus.

### 3.3. The optimization model inside the EMS

The developed EMS includes an optimization model to schedule plants and components optimally. The following sets have been used to formalize the optimization problem:

- $N = \{1, ..., N\}$ set of the grid nodes;
- $H_{F,i} = \{1, ..., N_{f,i}\}$ set of controllable plants at node *i;*
- $H_{R,i} = \{1, ..., N_{r,i}\}$ set of renewable plants at node *i;*
- $S_i = \{1, ..., N_{s,i}\}$ set of storage elements at node *i;*

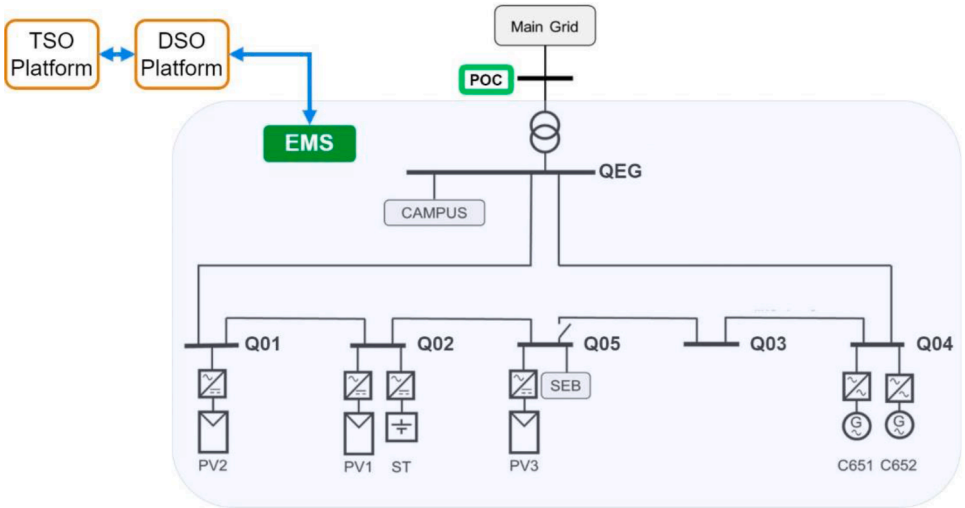


**Fig. 1.** Simplified one-line diagram of the Single PoC configuration considered in Scenario 1.

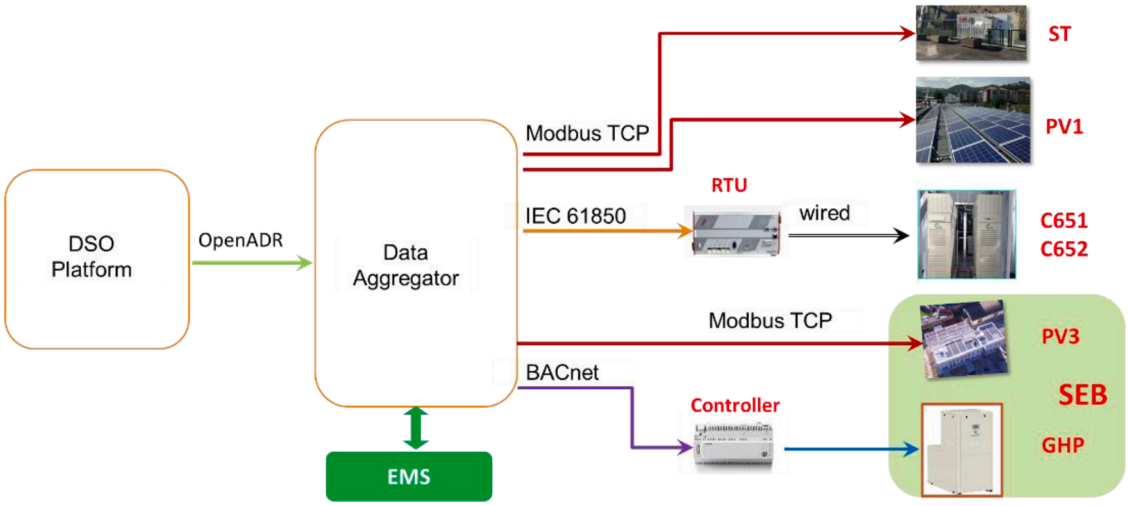


**Fig. 2.** Communication scheme relevant to the Single PoC configuration in Scenario 1.

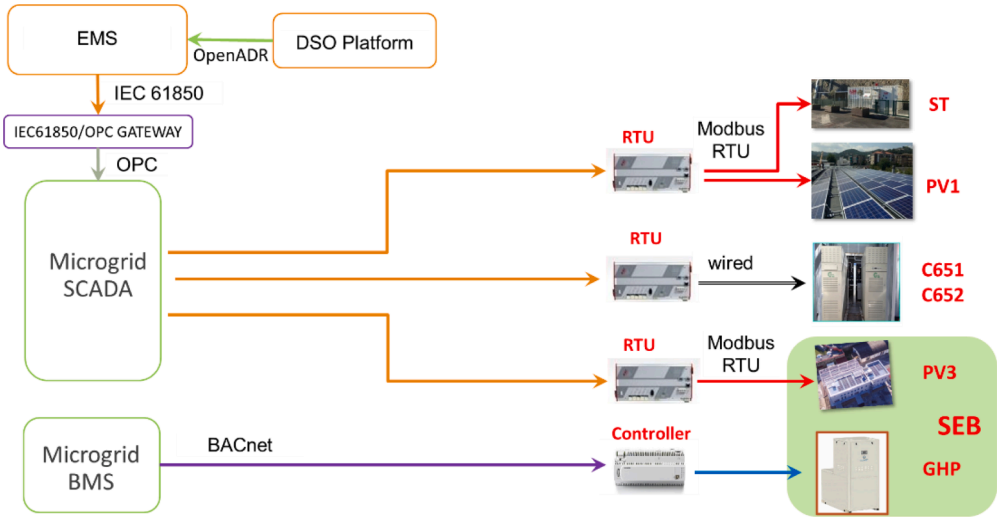


**Fig. 3.** Islanded mode communication scheme.

- $A_i = \{1, ..., n_i\}$ set of nodes connected to node $i$;
- $N_I = \{1, ..., n_I\}$ set of the grid nodes that can perform islanded mode operation.

The developed optimization model can be used under different cases in the Single-PoC scenario: (1) normal operation (i.e., costs are minimized and plants and storage systems scheduled, but equations and variables related to DR and islanding are not considered); (2) demand response (i.e., concerning normal operation 1) additional constraints are considered, at any request, as described in the following); (3) intentional islanding (two models manage the two sub-portions of the microgrid).

The overall optimization problem is given by:

$$\min f \tag{1}$$

**s.t.**

$$f = \sum_{t=0}^{T-1} \sum_{i \in N} \left\{ \Delta \left[ \begin{array}{l} \left(C_t + f_e C_{CO2,em}\right) P_{grid,IN,i,t} - B_t P_{grid,OUT,i,t} \\ + P_{PE,B,i,t} \left(C_{CO2,em} \widetilde{E}_{f-ng} + TES_{pp}\right) + C_{CO2,em} P_{PE,h,i,t} E_{f-ng} \end{array} \right] + \sum_{h=1}^{H_{F,i}} Q_{gas,h,i,t} C_{gas} \right\} \tag{2}$$

$$a^{MIN} D_{heat,t} \leq \sum_{i \in N} \sum_{h \in H_{F,i}} P_{th,h,i,t} + P_{th,B,t} + P_{th,RES,i,t} - P_{th,CHI,t} \leq a^{MAX} D_{heat,t} t = 0, ..., T-1 \tag{3}$$

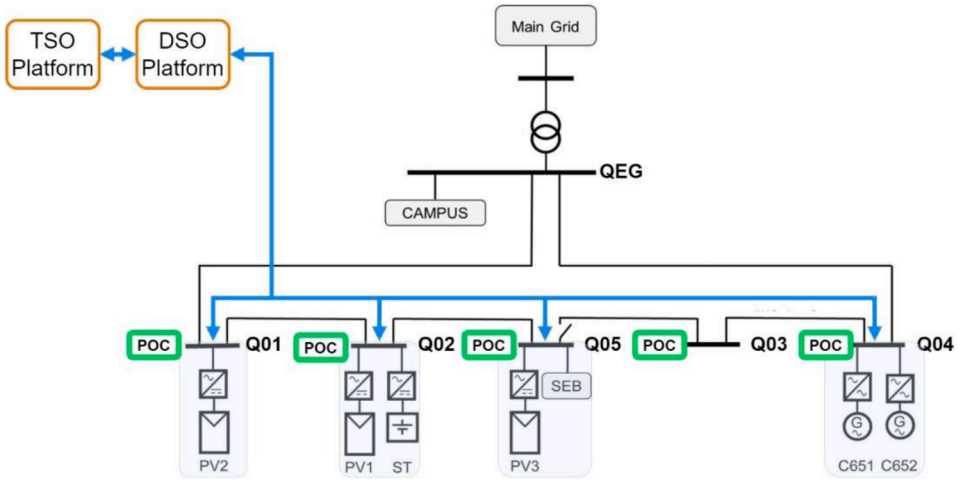


**Fig. 4.** Simplified one-line diagram of the Multi-PoC configuration considered in Scenario 2.

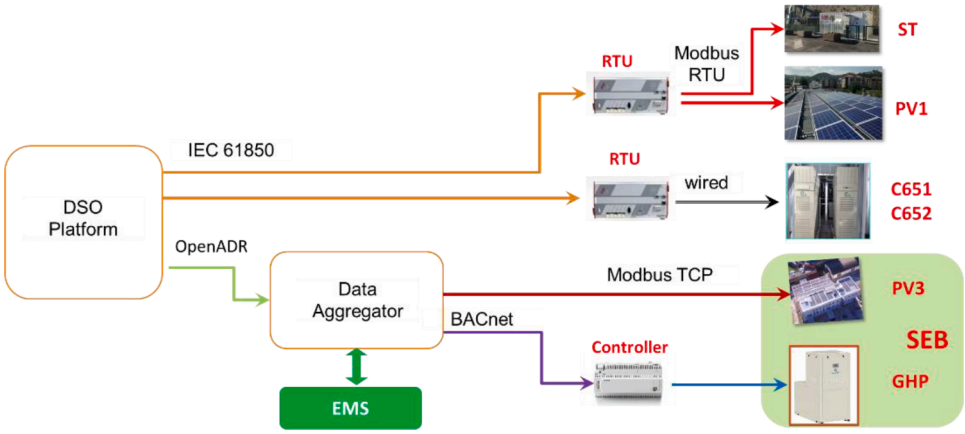


**Fig. 5.** Communication scheme relevant to the Multi PoC configuration in Scenario 2.

$$\chi P_{th,CHI,t} \geq D_{cool,t} t = 0, ..., T-1 \tag{4}$$

$$P_{PE,B,t}\eta_B = P_{th,B,t} t = 0, ..., T-1 \tag{5}$$

$$P_{PE,h,i,t}\eta_h = P_{th,h,i,t} h \in H_{F,i}, i \in N, t = 0, ..., T-1 \tag{6}$$

$$P_{th,h,i,t}\eta_{th,h} = P_{el,h,i,t} h \in H_{F,i}, i \in N, t = 0, ..., T-1 \tag{7}$$

$$P_{el,HP,i,t} COP_i = P_{th,HP,i,t}\, i \in N, \quad t = 0, \ldots, T-1 \tag{8}$$

$$P_{th,HP,i,t} = \frac{P_{th,FC,i,t}}{\eta_{FC,i}} i \in N, \quad t = 0, \ldots, T-1 \tag{9}$$

$$T_{build,i,t+1} = \frac{\left(\frac{T_{ext,t} - T_{build,i,t}}{R_{build,i}} + \alpha_{FC,i} P_{th,FC,i,t}\right)\Delta}{C_{build,i}} + T_{build,i,t} i \in N, \quad t = 0, \ldots, T-1 \tag{10}$$

$$\sum_{h \in H_{F,i}} P_{el,h,i,t} + \sum_{l \in H_{R,i}} P_{RES,l,i,t} - \sum_{k \in S_i} P_{S,k,i,t} - P_{D,i,t} + P_{grid,i,t} - P_{el,HP,i,t} - P_{veh,i,t} = \sum_{j \in A_i} P_{i,j,t} \quad i \in (N \setminus N_I),\ t = 0, \ldots, T-1 \tag{11}$$

$$\sum_{l \in H_{R,i}} Q_{RES,l,i,t} - \sum_{k \in S_i} Q_{S,k,i,t} - Q_{D,i,t} + Q_{grid,i,t} = \sum_{j \in A_i} Q_{i,j,t} i \in (N \setminus N_I),\ t = 0, \ldots, T-1 \tag{12}$$

$$\left(1-\delta_t^{IM}\right)\left[\sum_{h\in H_{F,i}} P_{el,h,i,t}+\sum_{l\in H_{R,i}} P_{RES,l,i,t}-\sum_{k\in S_i} P_{S,k,i,t}-P_{D,i,t}+P_{grid,i,t}-P_{el,HP,i,t}-P_{veh,i,t}\right]=\sum_{j\in A_i} P_{i,j,t}\, i\ \in N_I,\ t=0,\ldots,T-1 \tag{13}$$

$$\left(1-\delta_t^{IM}\right)\left[\sum_{l\in H_{R,i}} Q_{RES,l,i,t}-\sum_{k\in S_i} Q_{S,k,i,t}-Q_{D,i,t}+Q_{grid,i,t}\right]=\sum_{j\in A_i} Q_{i,j,t}\, i\ \in N_I,\ t=0,\ldots,T-1\, i\ \in N,\ t=0,\ldots,T-1 \tag{14}$$

$$P_{D,i,t}=P_{Diff,i,t}+P_{NDiff,i,t}\, i\ \in N,\ t=0,\ldots,T-1 \tag{15}$$

$$\sum_{t=1}^{T}\sum_{i\in N} P_{Diff,i,t}\Delta \geq D_{Diff,i}\, i\in N, t=0,\ldots,T-1 \tag{16}$$

$$p_{i,j,t}=G_{i,j}\left(v_{i,t}\right)^2-v_{i,t}v_{j,t}\left(G_{i,j}\cos\left(\delta_{i,t}-\delta_{j,t}\right)+B_{i,j}\sin\left(\delta_{i,t}-\delta_{j,t}\right)\right) i,j\ \in N,\ \ i\neq j,\ \ t=0,\ldots,T-1 \tag{17}$$

$$q_{i,j,t}=-B_{i,j}\left(v_{i,t}\right)^2-v_{i,t}v_{j,t}\left(-B_{i,j}\cos\left(\delta_{i,t}-\delta_{j,t}\right)+G_{i,j}\sin\left(\delta_{i,t}-\delta_{j,t}\right)\right) i,j\ \in N,\ \ i\neq j,\ \ t=0,\ldots,T-1 \tag{18}$$

$$p_{i,j,t}=\left[G_{i,j}\left(v_{i,t}\right)^2-v_{i,t}v_{j,t}G_{i,j}\cos\left(\delta_{i,t}-\delta_{j,t}\right)+v_{i,t}v_{j,t}B_{i,j}\sin\left(\delta_{i,t}-\delta_{j,t}\right)\right]\left(1-\delta_t^{IM}\right) i,j\ \in N_I,\ \ i\neq j,\ \ t=0,\ldots,T-1 \tag{19}$$

$$q_{i,j,t}=\begin{bmatrix}-B_{i,j}\left(v_{i,t}\right)^2+v_{i,t}v_{j,t}B_{i,j}\cos\left(\delta_{i,t}-\delta_{j,t}\right)\\ -v_{i,t}v_{j,t}G_{i,j}\sin\left(\delta_{i,t}-\delta_{j,t}\right)\end{bmatrix}\left(1-\delta_t^{IM}\right) i,j\ \in N_I,\ \ i\neq j,\ \ t=0,\ldots,T-1 \tag{20}$$

$$P_{RES,l,i,t}^2+Q_{RES,l,i,t}^2\leq S_{RES,l,i}^2 i\in N,\ \ l\in H_{R,i},\ \ t=0,\ldots,T-1 \tag{21}$$

$$P_{S,k,i,t}^2+Q_{S,k,i,t}^2\leq S_{S,k,i}^2 i\in N,\ \ k\in S_i,\ \ t=0,\ldots,T-1 \tag{22}$$

$$SOC_{k,i,t+1}=a_{k,i,t}SOC_{k,i,t}+\frac{\eta_{k,i,t}P_{S,k,i,t}\Delta}{CAP_S} i\in N,\ \ k\in S_i,\ \ t=0,\ldots,T-1 \tag{23}$$

$$\eta_{k,i,t}=\begin{cases}\eta_{c,k,i} & if\quad P_{S,k,i,t}>0\\ 1/\eta_{d,k,i} & otherwise\end{cases} i\in N,\ \ k\in S_i,\ \ t=0,\ldots,T-1 \tag{24}$$

The objective function (2) minimizes the operation costs of the SPM, also considering the emissions due to the gas consumption and to the energy absorbed by the main grid. In (2), $\Delta$ is the time discretization interval, $P_{grid,IN,t}$ and $P_{grid,OUT,t}$ [kW] represents the power injected into the microgrid and the power sold to the main grid, $P_{PE,B,i,t}$ [kW] is the power associated with the primary energy consumption of the boiler, $P_{PE,h,i,t}$ [kW] is the power associated with the primary energy consumption of the h-th controllable plant, $Q_{gas,h,i,t}$ [m3] is the volume of gas consumed by the h-th controllable plant, $C_t$ and $B_t$ [€/kWh] are the unitary prices for purchasing/selling energy, $TES_{pp}$ [€/kWh] is the unit price for primary energy to feed boilers, $C_{gas}$ [€/m3] is the price of natural gas, $f_e$ [tCO2/kWh] is the emission factor relevant to the power purchased from the grid, $C_{CO2,em}$ [€/tCO2] is the cost relevant to the emission of one ton of CO2, $\widetilde{E}_{f-ng}$ and $E_{f-ng}$ [tCO2/kWh] are emission factors relevant to fossil fuel use.

The thermal power balance is provided by (3) and (4): $D_{heat,t}$ [kW] and $D_{cool,t}$ [kW] are the power demand (heating and cooling); $a^{MIN}$ and $a^{MAX}$ are parameters that set how much the power request can be violated; $P_{th,h,i,t}$ [kW] is the thermal power from controllable plants $P_{th,RES,i,t}$ [kW] is the thermal power from renewable plants, $P_{th,CHI,t}$ [kW] is the power generated by chillers and $P_{th,B,t}$ is the thermal power from the boiler, $\chi$ is the thermal efficiency of the chiller.

Constraints (5) and (6) determine the conversion from the primary energy to the thermal power production through the efficiencies $\eta_B$ and $\eta_h$. Eq. (7) represent the relation between thermal power production and the electrical one in the controllable plants.

Constraints (8)-(10) describe the building thermal model: $P_{th,HP,i,t}$ and $P_{el,HP,i,t}$ are the thermal power generated and the electrical power absorbed by the GHPs, respectively coupled by the performance coefficient $COP_i$; $T_{build,i,t}$ is the building temperature modelled as RC circuits with$C_{build,i}$ [kWh/K] thermal capacity and $R_{build,i}$ [K/kW] [K] building's thermal resistance, $P_{th,FC,i,t}$ the thermal power of the ventilation systems; $T_{ext,t}$ [K] is the external temperature, $\eta_{FC,i}$ and $\alpha_{FC,i}$ are the efficiencies of the fan coils, the first is related to the conversion from the thermal power produced by the heat pump to the fan coils and the second from the fan coils to the building.

A binary decision variable ($\delta_t^{IM}$) is introduced to define the possibility that the microgrid operates in Islanded Mode (IM), respectively equal to 1 when IM occurs and 0 otherwise.

The power grid is described employing (11)–(24). In particular, (11)–(14) are the active/reactive power balances at each node $i$, $P_{D,i,t}$ [kW] is the power load, $P_{grid,i,t}$ [kW] is the power exchanged with the grid, $P_{veh,i,t}$ [kW] is the power consumptions of the electric vehicles, $P_{S,k,i,t}$ [kW] is the power exchanged with the storage. Moreover, $Q_{D,i,t}$ and $Q_{grid,i,t}$[kVAR] are the corresponding reactive powers ((13) and (14) are considered for islanded mode nodes), $Q_{RES,l,i,t}$ [kVAR] is the reactive power associated with renewables and $Q_{S,k,i,t}$ [kVAR] is the reactive power associated with the storage. Finally, $P_{i,j,t}$ [kW] and $Q_{i,j,t}$ [kVAR] are the power flows on line $(i,j)$. It is important to note that, thanks to (15), $P_{D,i,t}$ is composed of two terms, $P_{Diff,i,t}$ and $P_{NDiff,i,t}$ [kW], which represent deferrable and non-

deferrable portions of the load. Moreover, the overall deferrable energy must be greater than a certain minimum deferrable demand $D_{Diff,i}$.

Constraints (17) and (20) represent the p.u. equivalent of the power flow equations [37]: $p_{i,j,t}$ and $q_{i,j,t}$ are active and reactive powers, $G_{i,j}$ and $B_{i,j}$ are lines' parameters, $v_{i,t}$ and $\delta_{i,t}$ are voltage and phase at node *i*. Constraints (21) and (22) are circular capability for renewables and storages.

The storage systems dynamics are described by (23) and (24) where $SOC_{k,i,t}$ [kWh] is the state of charge of the storage. The charge and the discharge efficiencies are $\eta_{c,k}$ and $\eta_{d,k}$, while $CAP_{S,k}$ [kWh] is the capacity of the storage system.

It is important to note that all variables have upper and lower bounds, but these constraints are not reported for brevity.

The system can also operate during a DR event in which the grid operator requests a certain power exchange. The following constraints have to be added:

$$\beta_{i,t}P_{grid,i,t} = P^{DR}_{grid,i,t}\beta_{i,t} i \in N,\ t = 0, \ldots, T-1 \tag{25}$$

$$\beta_{i,t}Q_{grid,i,t} = Q^{DR}_{grid,i,t}\beta_{i,t} i \in N,\ t = 0, \ldots, T-1 \tag{26}$$

where $P^{DR}_{grid,i,t}$ and $Q^{DR}_{grid,i,t}$ are the active and reactive power reference values required by the system operator, and $\beta_{i,t}$ is a binary parameter that is equal to 1 during a demand response event and 0 otherwise.

Furthermore, if the DSO requests cannot be fulfilled, the impossibility of achieving the DR requirement is communicated to the DSO together with the allowable flexibility of the system, which is defined under the following optimization problem:

$$\min \quad J = \sum_{t=0}^{T-1}\left\{\sum_{i\in N}\left(P_{grid,i,t}\right)^2 + \left(Q_{grid,i,t}\right)^2\right\} i \in N,\ t = 0, \cdots, T-1 \tag{27}$$
$$\textbf{Subject to constraints}\ (3) - (26)$$

## 4. Optimal results and in field testing

Optimal results and in-field testing, reported in the following, are related to the application in the LIVING GRID pilot site (Savona Campus SPM).

### 4.1. optimal results

The optimization model described in the previous section has been implemented in MATLAB (through the YALMIP interface [38]) and the runtime to reach an optimal solution is less than one minute. In the following, two cases are considered to show the obtained results:

- *Case I*. Costs are minimized while meeting a demand response request of 70 kW for one hour.

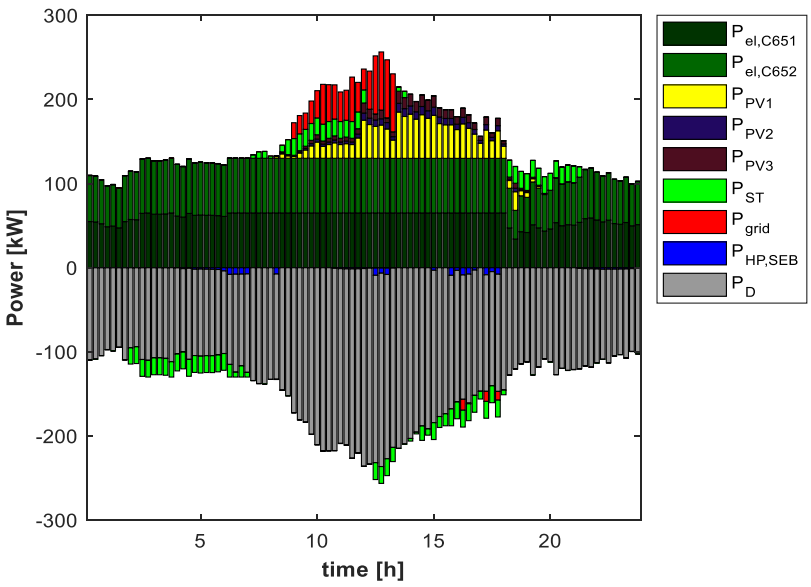


**Fig. 6.** . Scheduling of electrical power for the 24-h horizon without demand response.

- *Case II*. Costs are minimized while intentional islanding is performed for a portion of the SPM that is disconnected for a period of about 30 min.

#### 4.1.1. Case I

Demand response events consist of additional constraints whose validity must be met for certain time intervals. In this case, $P_{grid,i,t}$=70 kW from 13:15 to 14:15. The demand response constraint modifies in particular, the electrical scheduling and the state of charge of the battery.

Figs. 6 and 7 show the optimal results regarding the electric scheduling without and with demand response, respectively.

As it can be seen in Fig. 7, in the hour in which the constraint applies, the extra grid power is used to recharge the battery which reaches a higher state of charge than in the case shown in Fig. 6. Regarding the objective function, in the case demand response is performed, the cost increases from 466€ to 472€.

#### 4.1.2. Case II

In this case, a possible islanding mode of the SEB, the GHP, and the storage system has been considered. The new electrical and thermal scheduling in the winter scenario is then derived. Figs. 8 and 9 show the optimal values of the decision variables without and with the islanded operation.

In particular, with the islanded operation, the cost increases and is equal to 771€ (instead of 760€). This is because there is an increase in the power purchased from the network in the central hours of the day. The benefits of energy sales and the savings in demand of GHP are not enough to counteract the purchase costs.

### 4.2. In field testing

Field tests were carried out in two phases. A set of initial tests was scheduled at the end of July 2020, to validate the platform and to identify potential issues both in the commands sent by the platform following the requests of the users (DSO and TSO) and in the interaction between the platform and the devices at field level. Once all the issues arising during this phase were solved, the last experimental activity was carried out from September 2020 to the end of October 2020. Both the single-PoC and multi-PoC scenarios were tested during these two phases. In addition, the ability of a portion of the microgrid to safely perform the transition from on-grid to island (and vice versa) was also experimentally assessed.

In the following, some examples of the results will be discussed, in terms of the actual measured variables on the test-bed, in response to commands from the platform issued to comply with the requests from the DSO and TSO.

#### 4.2.1. Multi-PoC scenario - limits on the active and reactive power at the Q02 bus

This test enforced limits on the active and reactive powers on the bus Q02 (that hosts photovoltaic system PV1 and the storage

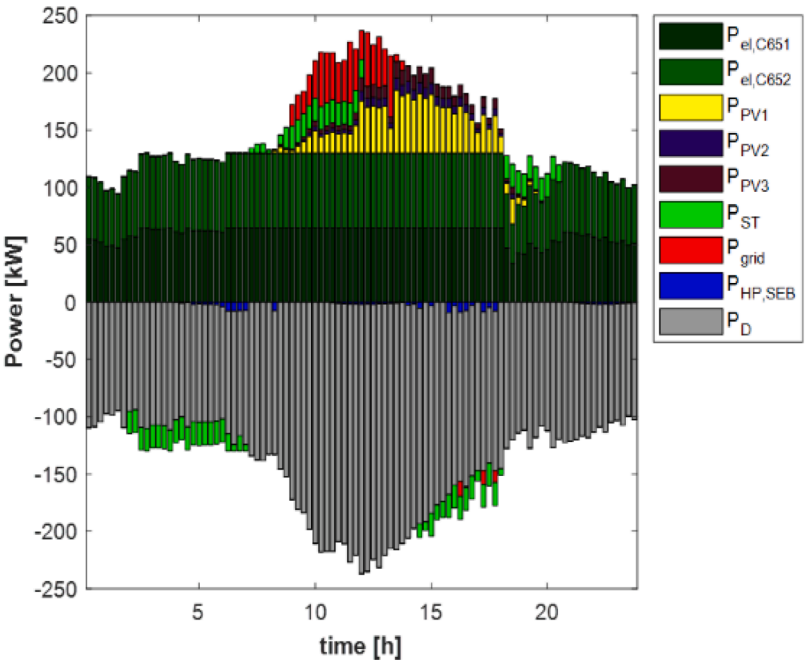


**Fig. 7.** . Scheduling of electrical power for the 24-h horizon with demand response.

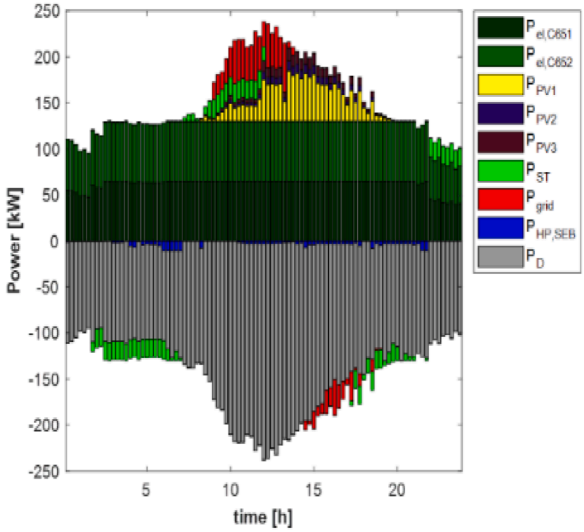


**Fig. 8.** Scheduling of electrical power for the 24-h horizon without islanding.

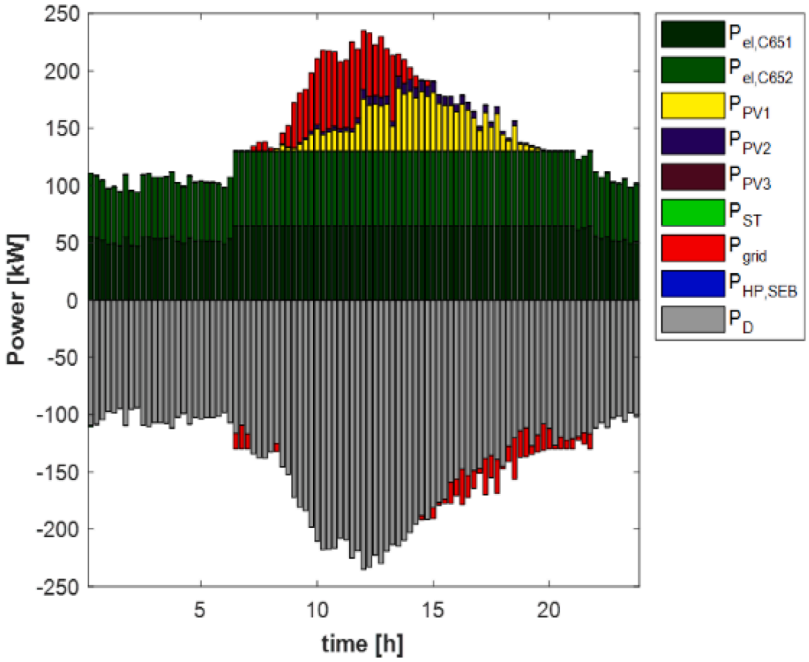


**Fig. 9.** Scheduling of electrical power for the 24-h horizon with islanding.

system). Specifically, maximum negative limits were specified (line in red in Fig. 10): since the passive sign convention is used for the powers exchanged by the bus, this corresponds to enforcing minimum generation requests for both the active and the reactive flows (Fig. 10).

The platform fulfils the constraint on the active power by using the storage system (Fig. 11), which compensates for a rather small production by PV1, due to the low radiation available during this period on the day of the test. Reactive power is injected by PV1 (Fig. 12).

Even if the platform computes the setpoints only based on forecasts, without any feedback, in this example the action succeeded in fulfilling the constraints. This is due to the reliability, for this specific day, of the forecast for both PV1 production and Q02 local load (this latter essentially due to auxiliary systems, so quite easy to forecast).

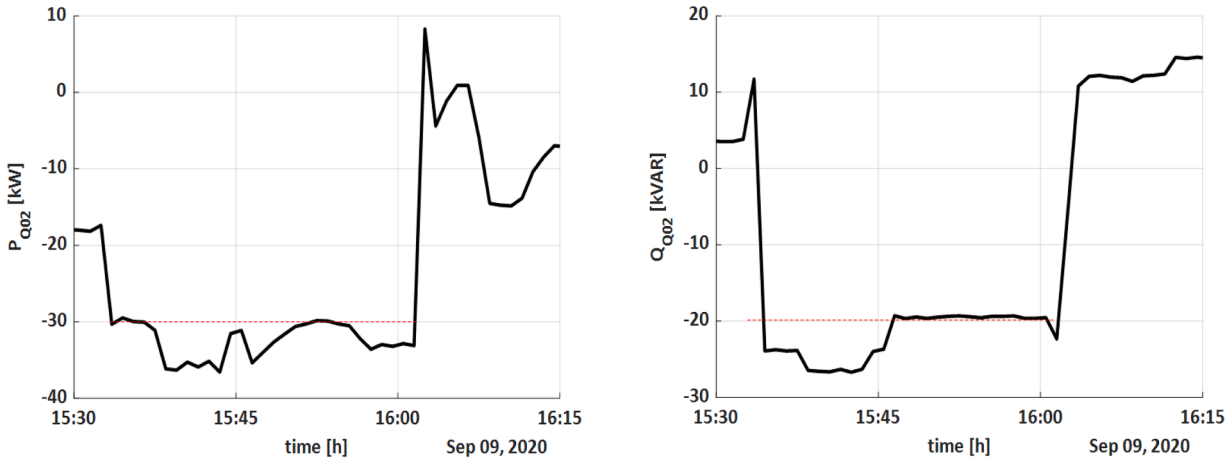


**Fig. 10.** Active and reactive power at bus Q02.

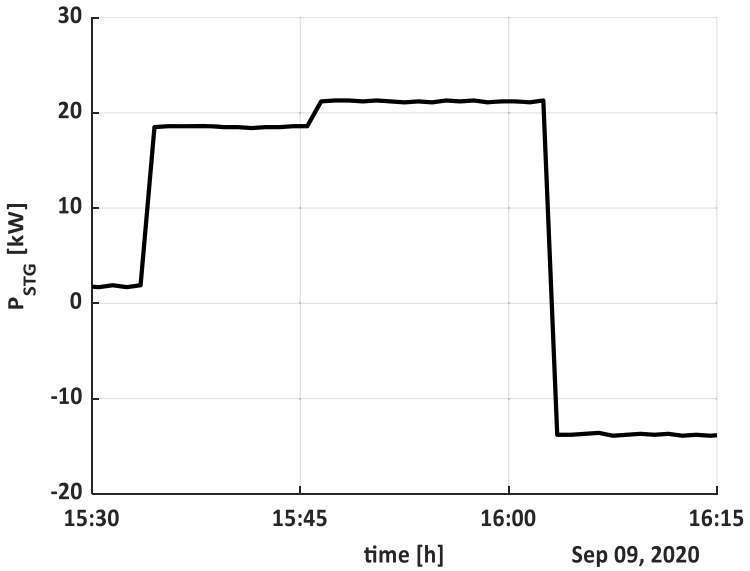


**Fig. 11.** Active power injected by the storage.

*4.2.2. Single-PoC scenario - limits on the active and reactive power fluxes at the POC*

In this test, the maximum values for the absorbed active and reactive power at the point of common coupling were specified, according to a TSO request, validated by the DSO. The request was relative to the period from 17:00 to 17:30. Given the forecasts for this period, a total reduction of about 40 kW (from 140 to 100 kW) for the active power and of 80 kVAR (from 100 to 20 kVAR) for the reactive power were needed (Fig. 13). The request was sent from the platform to the Aggregator, which triggered a new optimization to meet the specified constraints, considering the whole test-bed as a single entity (Single PoC scenario).

The EMS tried to meet the constraints by the following actions:

- a set point to the storage system of about 30 kW (power from the storage to the grid, Fig. 14a)
- a request to the SEB to maintain the GHP off in the considered period (this corresponds to a reduction of about 10 kW in the SEB load, Fig. 14b).

From the presented results, it is apparent that despite the assets following the prescribed setpoints, the limits at the PoC were met only partially. This is due to the following reasons:

- the forecasts for the active and reactive loads, based on which the optimization was performed, demonstrated a rather low accuracy, mainly because of two factors. Firstly, the forecasts were computed based on historical data of the previous years, related to operational conditions very different from the ones occurring in 2020 due to the COVID-19 pandemic (a partial lockdown was still

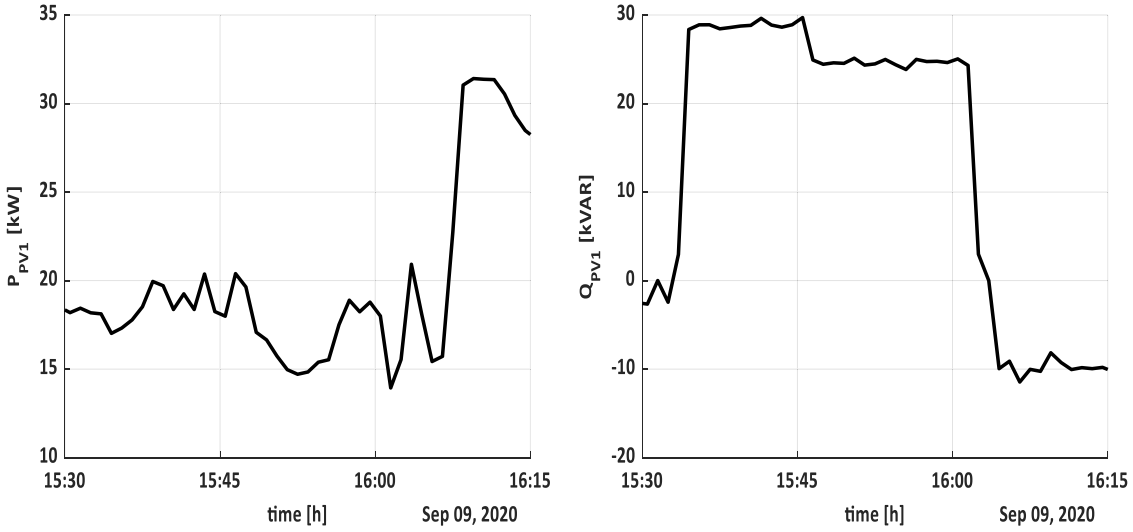


**Fig. 12.** Active and reactive power from PV1.

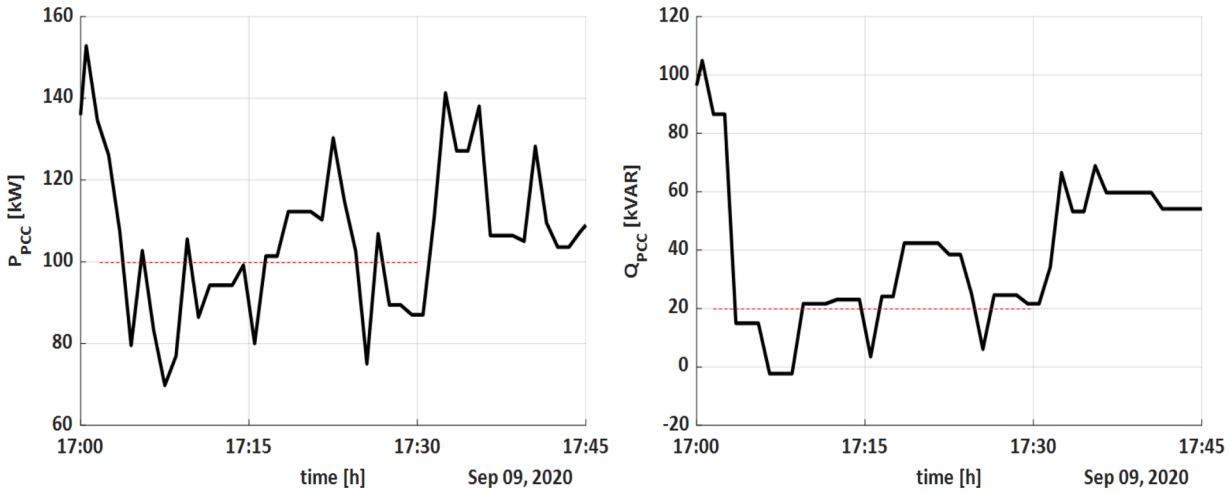


**Fig. 13.** Active and reactive power at the PoC.

in place, with remote lessons and smart working for the Campus personnel). Secondly, during the same period, due to another test, one of the laboratories of the Campus was absorbing an anomalous, rapidly varying load, between 10 and 100 kW, which further affected the reliability of the forecast.

- The SEB GHP was characterized by a very intermittent operation, due to the limited number of personnel in the SEB (due to the pandemic). This implied a limited thermal request and lowered reliability as a manageable load.

*4.2.3. Single-PoC scenario - reactive power bounds at the PoC*

This test was conceived to assess the ability of the test-bed, in the Single PoC scenario, to inject reactive power into the main network. Specifically, negative bounds for the reactive power (Fig. 15) were specified at the point of connection with the distribution network. The EMS met the request by specifying a set point of 10 kVAR for the storage system (Fig. 16a) and 30 kVAR for PV1 (Fig. 16b). The application of these set points led to an increase in the reactive power production of 40 kVAR and, thus, the inversion of the reactive power flow at the PoC.

The implementation of requests concerning the reactive power proved to be more reliable, as the forecasts for the reactive power were less susceptible to errors.

*4.2.4. Intentional islanding*

This test was intended to verify the ability of a section of the microgrid (switchboards Q01, Q02, and Q05), to perform a stable transition from grid-connected operation to islanding operation, following a request issued by the platform, to safely work

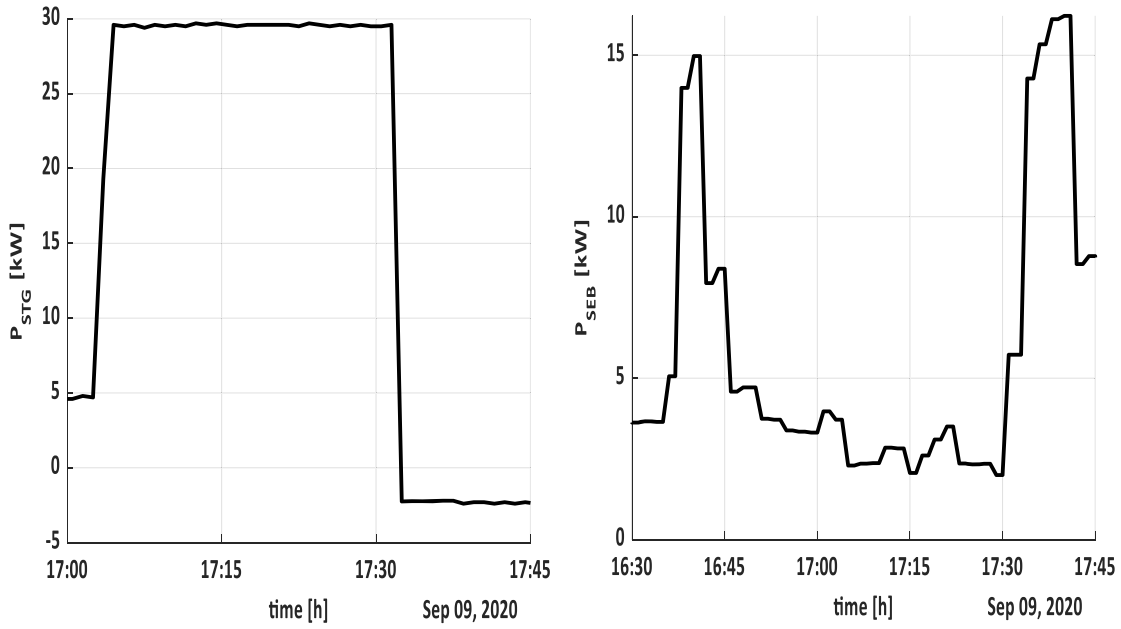


**Fig. 14.** (a) Active power injected by the storage system and (b) the GHP load of the SEB.

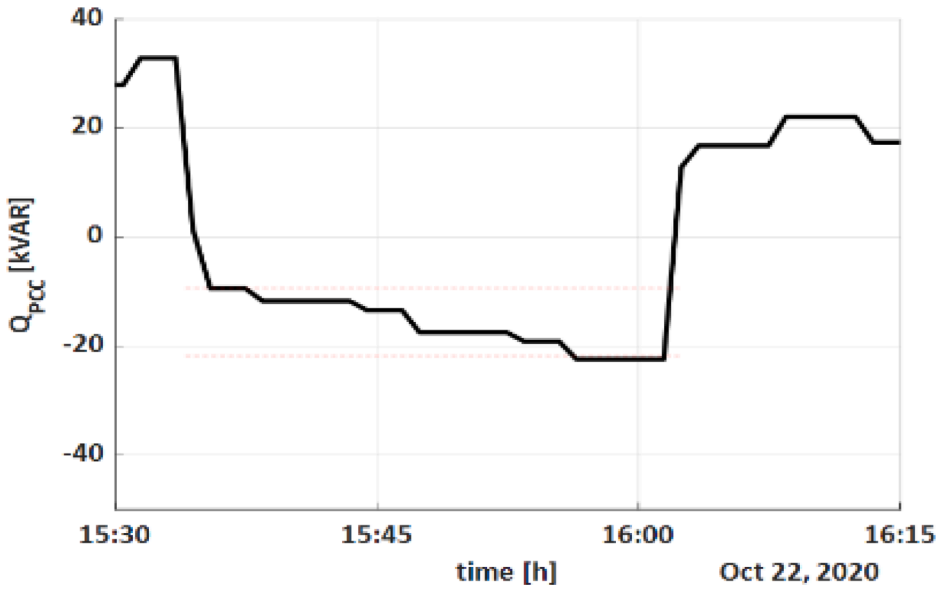


**Fig. 15.** Reactive power at the PoC.

disconnected from the main network for a given period, and then to reconnect to the main grid.

This feature was tested during the first set of tests at the end of July 2020. The islanding request, implemented as an IEC61850 command, was correctly received by the microgrid SCADA through a 61,850/OPC gateway. Upon the reception of the request, the islanding sequence was triggered:

- the storage system, usually operating in PQ mode (i.e., as a current source, exchanging an amount of reactive and active power with the network defined by the respective setpoints), stops; then, it switches to the "voltage source with droop" operation mode (i.e., acting as a voltage source, according to a given voltage-reactive power droop curve and a given frequency-active power droop curve) and restarts working in parallel with the main network;
- the photovoltaic generation is limited to avoid exceeding the maximum power the storage system can absorb, as when in islanding operation, the storage system acts as the network slack;

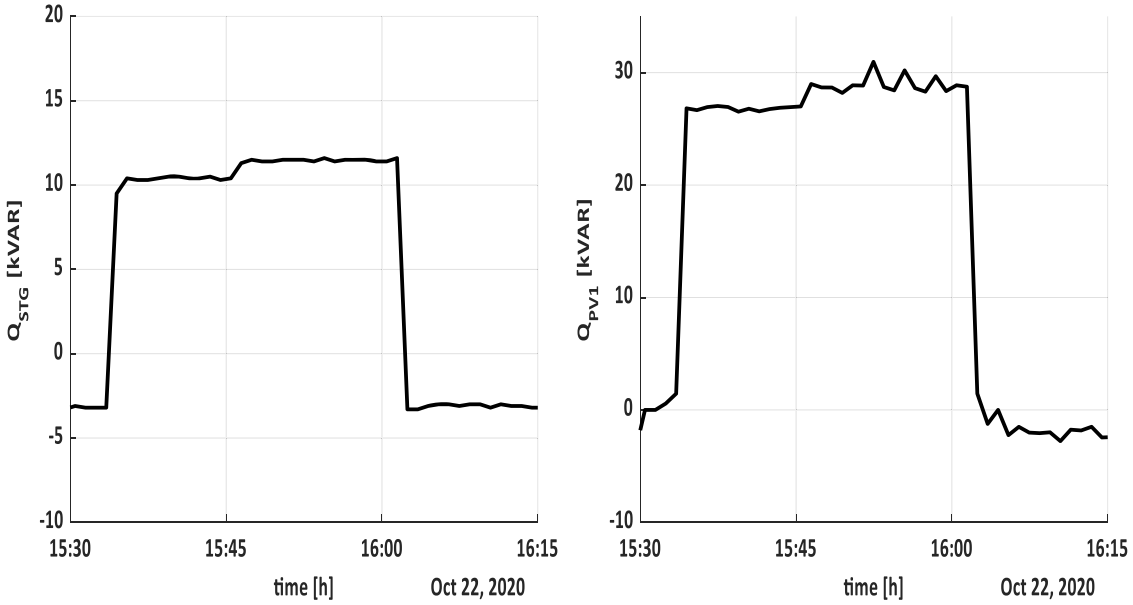


**Fig. 16.** Reactive power injected by (a) the storage and by (b) PV1.

- the breaker connecting Q01 with the main bus of the microgrid (QEG) is opened;
- since the microgrid is usually operated with the connection between Q05 and Q03 open (Fig. 1), Q01, Q02 and Q05 are now separated from the main grid.

When the request to reconnect to the main network is received, another sequence is triggered:

- acting on the reference voltage of the storage system, the RMS value of the microgrid voltages are adjusted to match the ones of the main network;
- a synchrocheck on the breaker connecting Q01 and QEG is activated and the frequency of the microgrid is tuned around the value of that of the main grid, acting on the frequency reference of the storage system;
- when the three-phase voltages of the islanded section are aligned to those of the main network, the breaker is closed;
- the storage system stops, switches back to PQ mode, and restarts.

Figs. 17–19a-b show the grid and island frequencies, one of the line-to-line voltages of the main grid and the corresponding voltage of the islanded network, the power exchanged through the connection between Q01 and QEG, and the active power of the storage: the

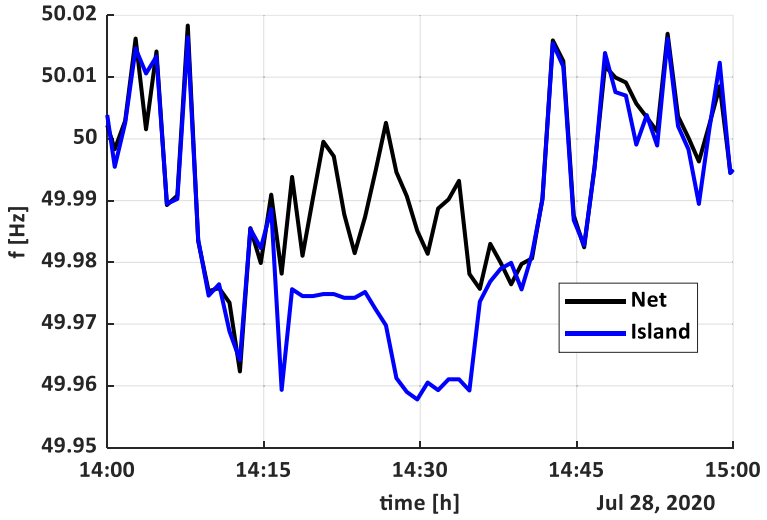


**Fig. 17.** Main net and island frequencies.

island voltages and frequency remain confined in acceptable ranges during the islanding mode operation and the transitions.

The outlined results show the technical feasibility of a purely software architecture that allows the TSO and DSO to request flexibility actions in a coordinated manner, and the prosumers to receive the requests and actuate them, both in the case of a "complex" prosumer, like a microgrid, equipped with a SCADA and an EMS (single-PoC scenario), and in the case of several simpler prosumers, equipped with assets such as PV, storage systems or manageable loads, like a GHP, all connected on the same distribution feeder (multi-PoC scenario).

From a practical point of view, the tests also highlighted that, for this scheme to work properly, reliable forecasts for the active and reactive power demands are crucial. In the performed tests, this proved to be especially true in the single-PoC scenario, as the load of the whole Campus was involved, which is harder to accurately predict, especially considering the discrepancy between the period in which the historical data were recorded and the actual situation of the Campus at the time of the tests, due to the restrictions of the COVID-19 pandemics. This situation affected also the predictability of the behaviour of the GHP installed in the SEB, thus limiting its reliability as a manageable load. Finally, the intentional islanding test showed the possibility, for a building equipped with PV and a storage device (initially installed to work in PQ mode but modified to be able to operate as a voltage source with droop also) to disconnect from the main network upon request and then safely reconnect: this feature could be exploited as an additional flexibility, for instances in case of contingencies on the distribution network.

## 5. Conclusion

An optimization-based ICT architecture developed as a joint effort of TSO, DSO and active local prosumers within the Italian LIVING GRID innovation and demonstration project, has been described. The main contributions of the paper regarding: the definition of the architecture of the platform jointly developed and tested by the main actors of the smart grid (TSO, DSO, active local prosumers) for demand response and intentional islanding, a new optimization model that allows selecting the optimal schedule of production plants and storage systems; the possibility to request the intentional islanding of a subset of the Microgrid; the testing in the field of the developed platform.

From a practical point of view, the concept of the platform and the experimental activity carried out in LIVING GRID was also inspired by an ongoing discussion at national level (at the time the project was conceived) about the Italian standards regulating the connection of active users to the public network. Specifically, the discussion concerned the requirement for the active user to install a central plant controller predisposed to exchange measures, information and commands with the DSO's grid control and supervision systems. The activity carried out during LIVING GRID was conceived as an attempt at practically testing a solution that did not require the installation of any additional physical control equipment at the user's premises, but was purely based on a software platform, simply interfaced with a typical supervision system of a microgrid or directly with the decentralized sources' controllers.

The field tests carried out during the project showed the technical feasibility of such an ICT infrastructure, especially from the point of view of the actual interface between the software platform and typical supervision and control systems at the prosumers' premises. Nevertheless, the tests also highlighted the necessity to better characterize the expected behaviour of the loads with reliable forecasts, based on historical values collected in a time span more correlated with the actual operating conditions in the period of interest.

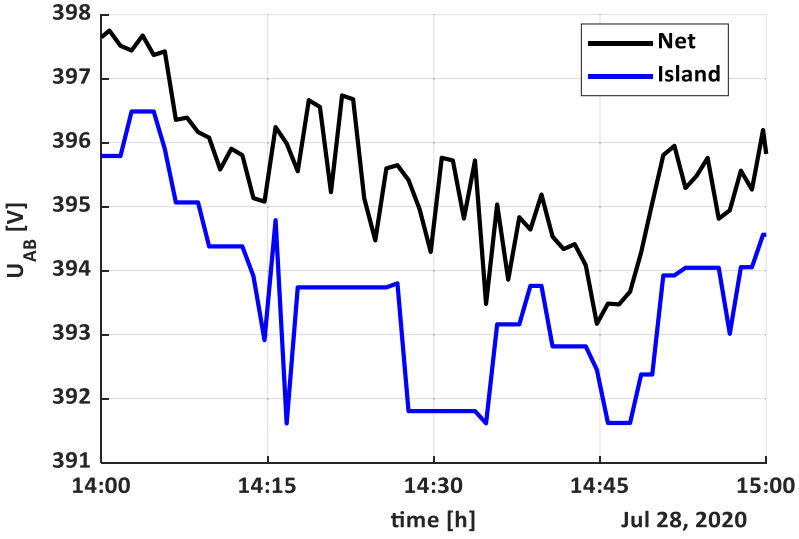


**Fig. 18.** Line to line voltages between phases A and B, measured at a bus belonging to the main network and at one belonging to the islanded portion of the microgrid.

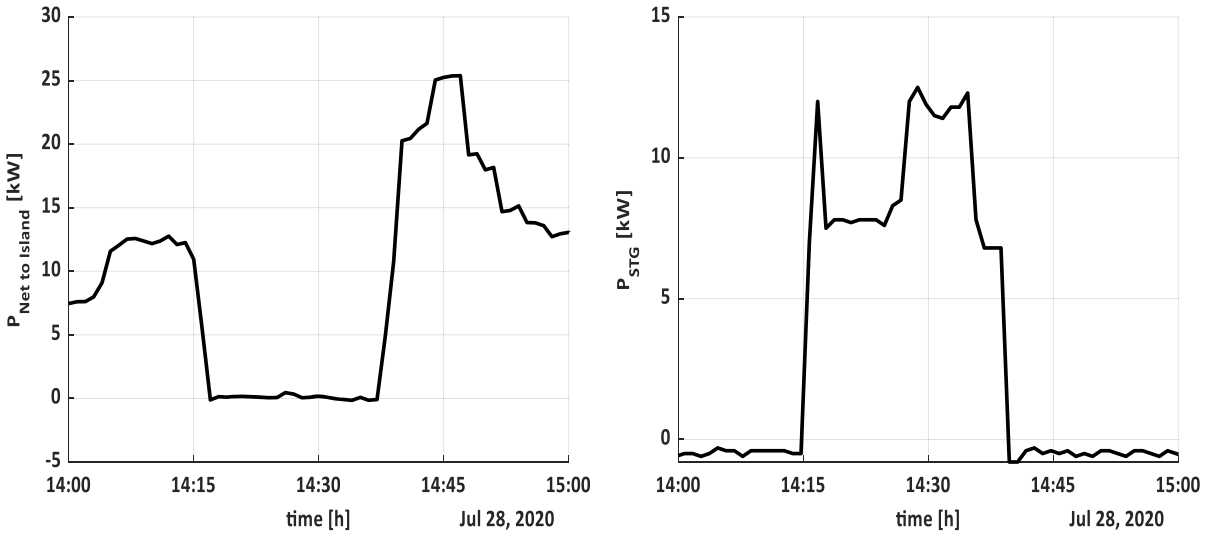


**Fig. 19.** (a) Power exchanged on the Q01-QEG link and (b) active power exchanged by the storage.

## Declaration of Competing Interest

The authors declare that they have no known competing financial interests or personal relationships that could have appeared to influence the work reported in this paper.

## Data availability

The authors do not have permission to share data.

## Acknowledgments

The work has been done thanks to the funds of the LIVING GRID project (2017–2020) from Italian Ministry of research (Innovation Technological Clusters).

## References

[1] Givisiez A, Petrou K, Ochoa L. A review on TSO-DSO coordination models and solution techniques. Electr Power Syst Res 2020;189:106659. https://doi.org/10.1016/j.epsr.2020.106659.
[2] Baltputnis K, Repo S, Mutanen A. The role of TSO-DSO coordination in flexibility asset prequalification. In: Proceedings of the 17th international conference on the European Energy Market (EEM); 2020. https://doi.org/10.1109/eem49802.2020.9221903.
[3] Savvopoulos N, Konstantinou T, Hatziargyriou N. TSO-DSO coordination in decentralized ancillary services markets. In: Proceedings of the international conference on Smart Energy Systems and Technologies (SEST); 2019. https://doi.org/10.1109/sest.2019.8849142.
[4] Grottum H, Bjerland S, del Granado P, Egging R. Modelling TSO-DSO coordination: the value of distributed flexible resources to the power system. In: Proceedings of the 16th international conference on the European Energy Market (EEM); 2019. https://doi.org/10.1109/eem.2019.8916377.
[5] Yohanandhan RV, Elavarasan RM, Pugazhendhi R, Premkumar M, Mihet-Popa L, Zhao J, Terzija V. A specialized review on outlook of future Cyber-Physical Power System (CPPS) test-beds for securing electric power grid. Int J Electr Power Energy Syst 2022;136. https://doi.org/10.1016/j.ijepes.2021.107720.
[6] Gulotta F, et al. Opening of the Italian ancillary service market to distributed energy resources: preliminary results of UVAM project. In: Proceedings of the IEEE 17th international conference on smart communities: improving quality of life using ICT, IoT and AI (HONET); 2020. p. 199–203. https://doi.org/10.1109/HONET50430.2020.9322822.
[7] Directive (EU) 2019/944 of the European Parliament and of the Council of 5 June 2019 on common rules for the internal market for electricity and amending Directive 2012/27/EU (2023).
[8] ARERA Resolution 352/2021/R/eel - Pilot projects for the procurement of local ancillary services (2023).
[9] Paredes A, Aguado JA. Capacity and energy local flexibility markets for imbalance and congestion management. In: Proceedings of the IEEE International Smart Cities Conference (ISC2); 2021. p. 1–7. https://doi.org/10.1109/ISC253183.2021.9562971.
[10] Bouloumpasis DS, Tuan LA. Congestion management using local flexibility markets: recent development and challenges. In: Proceedings of the IEEE PES Innovative Smart Grid Technologies Europe (ISGT-Europe); 2019. p. 1–5. https://doi.org/10.1109/ISGTEurope.2019.8905489.
[11] Ferro G, Minciardi R, Parodi L, Robba M, Rossi M. Optimal control of multiple microgrids and buildings by an aggregator. Energies 2020;13(5):1058. https://doi.org/10.3390/en13051058.
[12] Delfino F, Ferro G, Robba M, Rossi M. An energy management platform for the optimal control of active and reactive power in sustainable microgrids. IEEE Trans Ind Appl 2019. https://doi.org/10.1109/TIA.2019.2913532.
[13] Bianco G, Delfino F, Ferro G, Robba M, Rossi M. A hierarchical Building Management System for temperature's optimal control and electric vehicles' integration. Energy Convers Manag 2023;X, 17,:100339.
[14] Siano P. Demand response and smart grids - a survey. Renew Sustain Energy Rev 2014;30:461–78. https://doi.org/10.1016/j.rser.2013.10.022.
[15] Balijepalli VSKM, Pradhan V, Khaparde SA, Shereef RM. Review of demand response under smart grid paradigm. In: Proceedings of the IEEE PES international conference on innovative smart grid technologies ISGT India 2011; 2011. p. 236–43. https://doi.org/10.1109/ISET-India.2011.6145388.

[16] MacDonald J, Cappers P, Callaway D, Kiliccote S. Demand response providing ancillary services: a comparison of opportunities and challenges in us wholesale markets. Lawrence Berkeley National Laboratory; 2023.
[17] Shewale A, Mokhade A, Funde N, Bokde ND. An overview of demand response in smart grid and optimization techniques for efficient residential appliance scheduling problem. Energies 2020;13(6). https://doi.org/10.3390/en13164266.
[18] Khalili R, Khaledi A, Marzband M, Nematollahi AF, Vahidi B, Siano P. Robust multi-objective optimization for the Iranian electricity market considering green hydrogen and analyzing the performance of different demand response programs. Appl Energy 2023;334:120737.
[19] Ma K, Yao T, Yang J, Guan X. Residential power scheduling for demand response in smart grid. Int J Electr Power Energy Syst 2016;78:320–5. https://doi.org/10.1016/j.ijepes.2015.11.099.
[20] Astriani Y, Shafiullah GM, Shahnia F. Incentive determination of a demand response program for microgrids. Appl Energy 2021;292(March):116624. https://doi.org/10.1016/j.apenergy.2021.116624.
[21] Shehzad Hassan MA, Chen M, Lin H, Ahmed MH, Khan MZ, Chughtai GR. Optimization modeling for dynamic price based demand response in microgrids. J Clean Prod 2019;222:231–41. https://doi.org/10.1016/j.jclepro.2019.03.082.
[22] Nan S, Zhou M, Li G. Optimal residential community demand response scheduling in smart grid. Appl Energy 2018;210:1280–9. https://doi.org/10.1016/j.apenergy.2017.06.066.
[23] R. Singh, J. Reilly, A. Phan, E. Stein, D. Kotur, M. Petrovic, W. Allen, and M. Smith, "Microgrid energy management system integration with advanced distribution management system.", United States: N. p., 2020. Web. doi: 10.2172/1706120.
[24] Reilly JT. From microgrids to aggregators of distributed energy resources. The microgrid controller and distributed energy management systems. Electr J 2019; 32(5). https://doi.org/10.1016/j.tej.2019.05.007.
[25] Liu F, Chen C, Lin C, Li G, Xie H, Bie Z. Utilizing aggregated distributed renewable energy sources with control coordination for resilient distribution system restoration. IEEE Trans Sustain Energy 2023;14(2):1043–56.
[26] Wang J, Huang J, Zhou X. Performance evaluation of distributed energy resource management algorithm in large distribution networks. In: Proceedings of the IEEE power and energy society general meeting; 2021.
[27] Peppanen J, Deboever J, Coley S, Renjit A. Value of derms for flexible interconnection of solar photovoltaics. In: Proceedings of the CIRED. 20; 2021. p. 557–60. https://doi.org/10.1049/oap-cired.2021.0116. 2020.
[28] Fattahi J, Wright D, Schriemer H. An energy internet DERMS platform using a multi-level Stackelberg game. Sustain Cities Soc 2020;60. https://doi.org/10.1016/j.scs.2020.102262.
[29] Morrissey K, Ioan A. Optimal energy storage schedules for load leveling and ramp rate control in distribution systems. In: Proceedings of the IEEE conference on technologies for sustainability; 2020. p. 23–6. doi:.
[30] Seal Brian, Renjit A, Deaver B. Understanding derms. Electric Power Research Institute; 2018.
[31] N. Duan, N. Yee, B. Salazar, J.Y. Joo, E. Stewart, and E. Cortez, " Cybersecurity Analysis of distribution grid operation with distributed energy resources via co-simulation", 2020. doi: 10.1109/PESGM41954.2020.9281757.
[32] Majumdar A, Alizadeh-Mousavi O. Efficient distribution grid flexibility provision thorugh model-based MV grid and model-less LV grid approach. In: Proceedings of the CIRED conference Geneva; 2021. p. 20–3. 20 –23 September 2021.
[33] Ahmadi AR, Martinez I, Stojkovska B, Shaw R, Manandhar T, Georgiopoulos S. UK power networks providing power services from distributed energy resources to tansmission system operator via a centralised DERMS platform. In: Proceedings of the CIRED conference madrid; 2019. 3 –6 June10.34890/761.
[34] Padullaparti H, Pratt A, Mendoza I, Tiwari S, Baggu M, Bilby M, Ngo C. Peak load management in distribution systems using legacy utility equipment and distributed energy resources. In: Proceedings of the IEEE green technologies conference; 2021.
[35] Wang J, Padullaparti H, Veda S, Mendoza I, Tiwari S, Baggu M. Performance evaluation of data-enhanced hierarchical control for grid operations; performance evaluation of data-enhanced hierarchical control for grid operations. In: Proceedings of the IEEE Power & Energy Society General Meeting (PESGM); 2020. p. 1–5. https://doi.org/10.1109/PESGM41954.2020.9281456.
[36] Nowak S, Tehrani N, Metcalfe MS, Eberle W, Wang L. Cloud-based DERMS test platform using real-time power system simulation. In: Proceedings of the IEEE power and energy society general meeting. 2018-August; 2018. https://doi.org/10.1109/PESGM.2018.8585806.
[37] Kersting WH. Distribution system modeling and analysis. CRC Press; 2017.
[38] Lofberg Johan. YALMIP: a toolbox for modeling and optimization in MATLAB. In: Proceedings of the IEEE international conference on robotics and automation. IEEE; 2004. p. 284–9. https://doi.org/10.1109/CACSD.2004.1393890.